Sevoflurane improves circulatory function and pulmonary fibrosis in rats with pulmonary arterial hypertension through inhibiting NF-κB signaling pathway

X. ZHAO, X. BAI, J.-L. LI, S.-M. LI, J. XI

Department of Cardiovascular Surgery, Qilu Hospital of Shandong University, Jinan, China

Abstract. – **OBJECTIVE:** The aim of this study was to explore the influences of sevoflurane inhalation therapy on circulation function and pulmonary fibrosis in rats with pulmonary arterial hypertension (PAH) and the nuclear factor-κB (NF-κB) signaling pathway.

MATERIALS AND METHODS: A total of 30 adult male Sprague-Dawley rats were randomly divided into three groups, including control group (CTL group, n=10), PAH group (n=10), and PAH + sevoflurane group (n=10) using a random number table. Subsequently, the pulmonary artery right ventricular systolic pressure (RVSP) and right ventricular hypertrophy index (RVHI) were measured. Rats in PAH group were subcutaneously injected with 60 mg/kg monocrotaline once to establish the model of PAH. 28 d later, the differences in the morphology of pulmonary tissues and the protein expression levels of phosphorylated inhibitory κB (p-IκB), p-P65, P65, cyclin D1, proliferating cell nuclear antigen (PCNA) and tubulin among the three groups were analyzed via hematoxylin-eosin (HE) staining and Western blotting, respectively. Meanwhile, the messenger ribonucleic acid (mRNA) expression level of P65 was determined via Reverse Transcription-quantitative Polymerase Chain Reaction (RT-qPCR). Additionally, changes in the expression levels of Ki-67 and α-smooth muscle actin (α-SMA) in rat pulmonary tissues of the three groups were evaluated through immunohistochemistry.

RESULTS: According to HE staining results, compared with CTL group, rats in PAH group exhibited significant thickening of the pulmonary artery wall, reduction of the vascular lumen, inflammatory cell infiltration, and thrombosis in some small arteries. This indicated that the PAH model was successfully established in rats. Compared with PAH group, PAH + sevoflurane group showed a significantly improved morphology of rat pulmonary tissues. Western blotting demonstrated that the protein expression levels of p-IκB, p-P65, and P65 in rat pulmonary tissues of PAH group were remarkably higher than CTL group ($p<0.01$). However, they were notably down-regulated in PAH + sevoflurane group when compared with those in PAH group ($p<0.05$). The above experimental results suggested that the NF-κB signaling pathway in pulmonary tissues of rats in PAH group was activated and was inhibited by sevoflurane. Subsequent RT-qPCR results indicated that no significant (N.S.) differences were observed in the mRNA level of P65 among the three groups. Compared with CTL group, PAH group showed significantly up-regulated levels of Ki-67 and α-SMA in rat pulmonary tissues ($p<0.01$). However, their expression levels were markedly reduced in PAH + sevoflurane group when compared with PAH group ($p<0.05$). Finally, the detection of pulmonary circulatory function-related indicators illustrated that RVSP and RVHI increased significantly in PAH group in comparison with CTL group. However, they declined remarkably in PAH + sevoflurane group when compared with those in PAH group ($p<0.05$).

CONCLUSIONS: Sevoflurane down-regulates the levels of p-IκB, p-P65, and P65 to repress the activation of the NF-κB signaling pathway. This may reduce pulmonary fibrosis and ultimately prevent PAH.

Key Words:
    Sevoflurane, NF-κB signaling pathway, Pulmonary arterial hypertension (PAH).

Abbreviation

Pulmonary arterial hypertension (PAH); right ventricular systolic pressure (RVSP); pulmonary artery smooth muscle cells (PASMCs); nuclear factor-κB (NF-κB); Sprague-Dawley (SD); Hematoxylin-Eosin (HE); radioimmunoprecipitation assay (RIPA); phenylmethylsulfonyl fluoride (PMSF); bicinchoninic acid (BCA); sodium dodecyl sulfate-polyacrylamide gel electrophoresis (SDS-PAGE); polyvinylidene difluoride (PVDF); Tris-Buffered Saline with Tween-20 (TBST); enhanced chemiluminescence (ECL); Messenger Ribonucleic Acid (mRNA); Reverse Transcription-Polymerase Chain Reaction (RT-PCR); Phosphate-Buffered Saline (PBS);

Corresponding Author: Jie Xi, MM; e-mail: xijie@sdu.edu.cn

α-smooth muscle actin (α-SMA); standard error of the mean (SEM); phosphorylated inhibitory κB (p-IκB); IκB kinase (IKK); tumor necrosis factor (TNF); proliferating cell nuclear antigen (PCNA).

Introduction

Pulmonary arterial hypertension (PAH) is a progressive and incurable disease. Its main pathological mechanism is that pulmonary vascular resistance and persistent elevation of pulmonary arterial pressure are caused by aberrant proliferation of endothelial cells. This may lead to elevated right ventricular systolic pressure (RVSP) and right ventricular hypertrophy, ultimately resulting in right heart failure and death[1-3]. The pathogenesis of PAH involves persistent vasoconstriction, vascular remodeling, and *in situ* thrombosis. Scholars[,5] have reported that abnormal proliferation of pulmonary artery smooth muscle cells (PASMCs) affects vascular remodeling, thereby playing a crucial role in the onset of PAH. Additionally, the nuclear factor-κB (NF-κB) signaling pathway is aberrantly activated in the PAH model. Currently, the main treatment agents for PAH include prostaglandins, PDE5 inhibitor, and endothelial receptor agonist. However, due to limited efficacy, current treatments can only partly alleviate the symptoms of PAH.

Sevoflurane, as a novel anesthetic, exhibits certain superiority in cardiovascular anesthesia. Its perioperative application has been confirmed to relieve myocardial ischemia and protect cardiac function. Meanwhile, it can mitigate myocardial ischemia-reperfusion injury in cardiopulmonary resuscitation patients[6-9]. However, the cardioprotective mechanism of sevoflurane in PAH has been rarely elucidated. Furthermore, whether such a mechanism depends on the influence on NF-κB signaling pathway remains to be deeply studied. Therefore, the aim of the present work was to explore whether sevoflurane produced a positive effect on the circulatory function of PAH rats *via* the NF-κB signaling pathway.

Materials and Methods

Animal Feeding, Treatment, and Grouping

A total of 30 male Sprague-Dawley (SD) rats weighing 175-200 g were fed in the specific pathogen-free animal room under a 12/12 h light-dark cycle. All rats were given free access to food and water. Experimental rats were randomly assigned into three groups, namely control group (CTL group), PAH group, and PAH + sevoflurane group. This research was approved by the Ethics Committee of Qilu Hospital of Shandong University.

Establishment of PAH Model and Drug Administration

Rats in PAH group and PAH + sevoflurane group were subcutaneously injected with 60 mg/kg monocrotaline once to construct the model of PAH. Subsequently, rats in PAH group were fed for another 28 d. Meanwhile, rats in PAH + sevoflurane group were administrated with 1.5% sevoflurane *via* inhalation daily for 28 d.

Hematoxylin-Eosin (HE) Histological Staining

Rats were first sacrificed *via* cervical spine dissection. Subsequently, the skin and subcutaneous tissues were cut open along the sternal midline using dissecting scissors disinfected with 75% alcohol. The ribs in the right of the sternum were cut off to separate and collect intact pulmonary tissues. Next, the tissues were rinsed with normal saline to remove residual blood therein, dried using filter paper, and weighed. 5 mm-thick tissues were then obtained using a blade. After fixing with 10% neutral formaldehyde solution for 24 h, the tissues were dehydrated and blocked. Meanwhile, the resulting tissues measuring 2.5×1.5×1.5 cm (thickness × length × width) were obtained. After that, they were placed in an embedding cassette, dehydrated, soaked, and embedded in paraffin. Prior to sectioning, paraffin-embedded tissue samples were frozen at –20°C and sliced into 5 μm-thick sections when the tissues were hard to a certain degree.

Tissues sections were first baked in an oven at 64°C for 45-50 min. Then, they were de-paraffinized in hot xylene (I) at 64°C, xylene (II), and xylene (III) separately for 5 min. After that, they were hydrated in absolute alcohol (I), absolute alcohol (II), 95% ethanol, 85% ethanol, and 75% ethanol, with each for 2 min respectively. After washing slightly with water for 1-2 min, tissue sections were stained with hematoxylin solution for 4 min. Then, they were washed again with running water for 2 min to clear away the hematoxylin solution. Later, the sections were treated with 1% hydrochloric acid alcohol for 5 s, slightly washed with water for 5 s, and treated with bluing reagent for 5-10 s. After rinsing with running water for 2 min, the resulting sections were stained with 0.5% eosin solution for 3 min, followed by washing with distilled water for 1-2 s.

Subsequently, the sections were dehydrated in 80% ethanol, 95% ethanol, and absolute alcohol for 15-30 s, 15-30 s, and 4 min, respectively. After transparentized in xylene (I) and (II) for 4 min each, they were sealed in neutral resin. Finally, the sections were photographed under a microscope. The images of tissue samples were acquired and analyzed using the Leica Application Suite imaging system.

Detection of the NF-κB Signaling Pathway in Pulmonary Tissues via Western Blotting

Tissue lysis buffer was prepared using an appropriate volume of radioimmunoprecipitation assay (RIPA) evenly mixed with phenylmethylsulfonyl fluoride (PMSF) at 100:1 (Beyotime, Shanghai, China). Pulmonary tissues were collected from rats of the three groups. After adding with the lysis buffer at 1: 10, the tissues were homogenized on ice using a tissue homogenizer for 5 min, followed by centrifugation at 4°C and 14,000 rpm for 30 min. The protein supernatant was then aspirated and subjected to a heat bath at 95°C for 10 min for protein denaturation. The prepared protein samples were stored in a refrigerator at −80°C for use, and the concentration of protein samples was quantified using the bicinchoninic acid (BCA) kit (Pierce, Rockford, IL, USA). After that, protein samples were separated by sodium dodecyl sulfate-polyacrylamide gel electrophoresis (SDS-PAGE) under the constant voltage of 80 V for 2.5 h and transferred onto polyvinylidene difluoride (PVDF) membranes (Millipore, Billerica, MA, USA) by the semi-dry transfer method. Once immersed in Tris-Buffered Saline with Tween-20 (TBST) buffer containing 5% skim milk powder and shaken slowly using a shaker, the membranes were incubated with primary antibodies overnight. On the next day, the membranes were incubated with corresponding secondary antibody at room temperature for 2 h, followed by washing with TBST twice and TBS once (10 min/time). Immunoreactive bands were exposed by the enhanced chemiluminescence (ECL) reagent in a darkroom. Finally, the relative expression level of proteins was analyzed using Adobe Photoshop software.

Measurement of Messenger Ribonucleic Acid (mRNA) Level of P65 Using Reverse Transcription-Polymerase Chain Reaction (RT-PCR)

Total RNA was extracted from tissues in the three groups using TRIzol reagent (Invitrogen, Carlsbad, CA, USA). The concentration of extracted RNA was measured using 2000 D ultraviolet spectrophotometer (Thermo Fisher Scientific, Waltham, MA, USA). Absorbance at 260 nm (A_{260}) was determined, and the ratio of A_{260}/A_{280} was taken as the indicator of RNA purity. Only those samples with A_{260}/A_{280} greater than 1.8 were used for subsequent investigations. Additionally, the quality of RNAs was evaluated via electrophoresis in 1% agarose gel stained with EtBr, namely the 28S and 18S bands were assessed. RNA samples with the 28S/18S ratio of 2:1 were used in RT-quantitative PCR (qPCR).

RT and qPCR were performed to detect the mRNA expression of P65 in rat pulmonary tissues of the three groups. In reverse transcriptase reaction, 500 ng of total RNA was divided into three portions and diluted by 10 folds, 3 μL of which was used for PCR amplification. The amplification level of the target gene was determined via 5% agarose gel electrophoresis. LabWorks 4.0 image acquisition and analysis software were adopted for quantification and data processing. To obtain reliable data, the above operations were performed in triplicate in each group. In the present study, the relative mRNA expression level of P65 was analyzed using the $2^{-\Delta\Delta Ct}$ method. Primer sequences used in this study were shown in Table I.

Immunohistochemistry

Paraffin-embedded sections were prepared by the same method as HE staining. After washing with phosphate-buffered saline (PBS) twice (5 min/time), the sections were added with 0.01 M sodium citrate buffer (pH=6.0) and boiled at about 95°C. Subsequently, the sections were placed in a boiling pot and boiled for 10-15 min until the effect of antigen retrieval was achieved, 3% BSA blocking solution was prepared using PBS (pH=7.4). Next, the sections in PBS were placed in the blocking solution and incubated for 30-60

Table I. Primer sequences.

Gene name	Forward sequence (5'-3')	Reverse sequence (5'-3')
P65	CACCAAAGACCCACCTCACC	CCGCATTCAAGTCATAGTCCC
β-actin	GCAGAAGGAGATTACTGCCC	GCTGATCCACATCTGCTGGAA

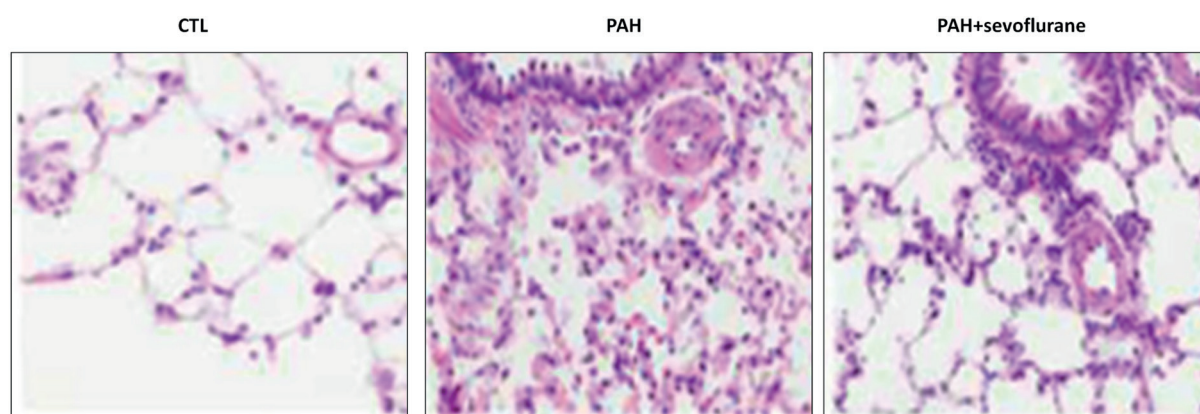**Figure 1.** Morphological differences of rat pulmonary tissues among the three groups analyzed *via* HE staining (magnification × 40).

min at room temperature. After that, they were incubated with α-smooth muscle actin (α-SMA) antibody diluted at 1:100 with blocking solution in a refrigerator at 4°C overnight. TBS (pH=7.4) was prepared and used to dilute AP-labeled anti-rabbit secondary antibody at 1:1000. The sections were then incubated with prepared AP-labeled anti-rabbit secondary antibody at room temperature for 2 h. The sections were washed with TBS (pH=7.4) for 3 times (with 5 min for each) to remove the secondary antibody, and the buffer was discarded. Each piece of section was added with no less than 100 μL of developer in the dark. Once the color was developed, the reaction was terminated by adding distilled water. Finally, the sections were counterstained with hematoxylin for 10 min, washed clean, covered with coverslips, observed, and photographed.

Statistical Analysis

GraphPad Prism 6.0 (La Jolla, CA, USA) was used for all statistical analysis. Experimental data were expressed as mean ± standard error of the mean (SEM). The *t*-test was used to compare the differences between the two groups. $p<0.05$ was considered statistically significant.

Results

Differences in the Morphology of Rat Pulmonary Tissues Among the Three Groups Analyzed via HE Staining

According to HE staining results, compared with CTL group, rats in PAH group exhibited significantly thickening of the pulmonary artery wall, reduction of the vascular lumen, inflammatory cell infiltration, and thrombosis in some small arteries. This indicated that PAH model was successfully established in rats. Moreover, PAH + sevoflurane group showed a significantly improved morphology of rat pulmonary tissues compared with PAH group (Figure 1).

Influence of Sevoflurane on the NF-κB Signaling Pathway

Western blotting indicated that the protein expression levels of phosphorylated inhibitory **κB** (p-IκB), p-P65, and P65 in rat pulmonary tissues of PAH group were remarkably up-regulated in comparison with CTL group ($p<0.01$). However, they were notably lower in PAH + sevoflurane group than those of PAH group ($p<0.05$). The above experimental results suggested that the NF-κB signaling pathway in the pulmonary tissues of PAH group was activated, which was repressed by sevoflurane (Figure 2).

Impact of Sevoflurane on the mRNA Expression Level of P65 in the Pulmonary Tissues

RT-qPCR results indicated that there were no significant (N.S.) differences in the mRNA expression of P65 in rat pulmonary tissues among the three groups (Figure 3).

Ki-67 Positive Rate in Pulmonary Tissues

Furthermore, Ki-67 positive rate of PASMCs was measured *via* immunohistochemistry. The results showed that PAH group showed a significantly higher level of Ki-67 than CTL group. However, PAH + sevoflurane group exhibited a remarkably lower Ki-67 positive rate than PAH group. These results implied that there were more
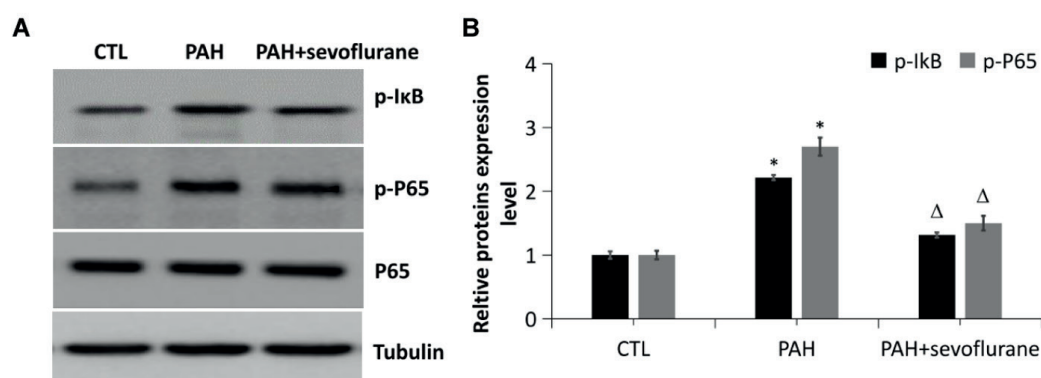
Figure 2. Influence of sevoflurane on the NF-κB signaling pathway. *A,* Expression levels of p-IκB, p-P65, P65, cyclin D1 and tubulin proteins. *B,* Quantified protein expression results. Note: Data were expressed as mean ± SEM, * PAH group *vs.* CTL group, $p<0.01$, and ᐃPAH + sevoflurane group *vs.* PAH group, $p<0.05$.

Ki-67-positive cells in pulmonary tissues in PAH group. Furthermore, sevoflurane prevented the increase in such PASMCs (Figure 4)

PASMC Proliferation-Related Factors in Pulmonary Tissues

Proteins in pulmonary tissues were extracted in the present study, and the expression levels of cell proliferation-related proteins were determined using Western blotting. The results illustrated that the expression level of cell cycle promoting protein cyclin D1 was significantly up regulated in PAH group compared with CTL group, thus promoting the proliferation of PASMCs. Compared with PAH group, the expression level of cyclin D1 was notably reduced by sevoflurane in PAH + sevoflurane group, thus inhibiting the proliferation of PASMCs. These findings were consistent with the results of immunochemistry (Figure 5).

Pulmonary Fibrosis Detected in Pulmonary Tissues

Immunochemical staining was then performed for α-SMA in pulmonary cells. It was found that PAH group showed a remarkably higher level of α-SMA than CTL group. However, PAH + sevoflurane group exhibited a significantly lower α-SMA positive rate than PAH group. All the above findings implied that pulmonary arterial vascular fibrosis occurred in PAH group, which was inhibited by sevoflurane (Figure 6).

Pulmonary Arterial Circulatory Function-Related Indicators

Arterial circulatory function indicators, including RVSP and right ventricular hypertrophy index (RVHI), were detected. The results showed that PAH group exhibited significantly larger RVSP and RVHI values than CTL group. How-
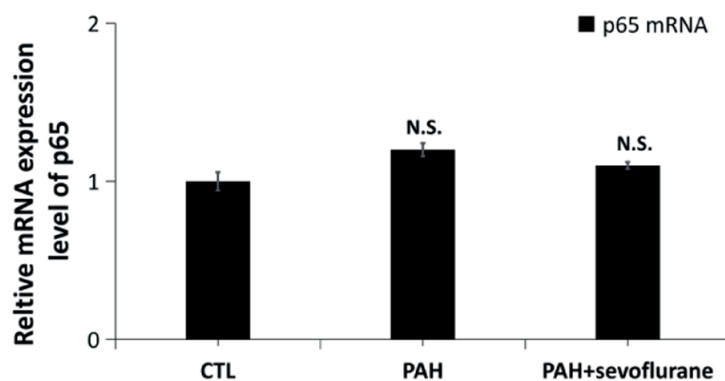

Figure 3. Impact of sevoflurane on the mRNA expression level of P65 in pulmonary tissues. Note: N.S.: there were no statistically significant differences among the three groups. Data were expressed as mean ± SEM.
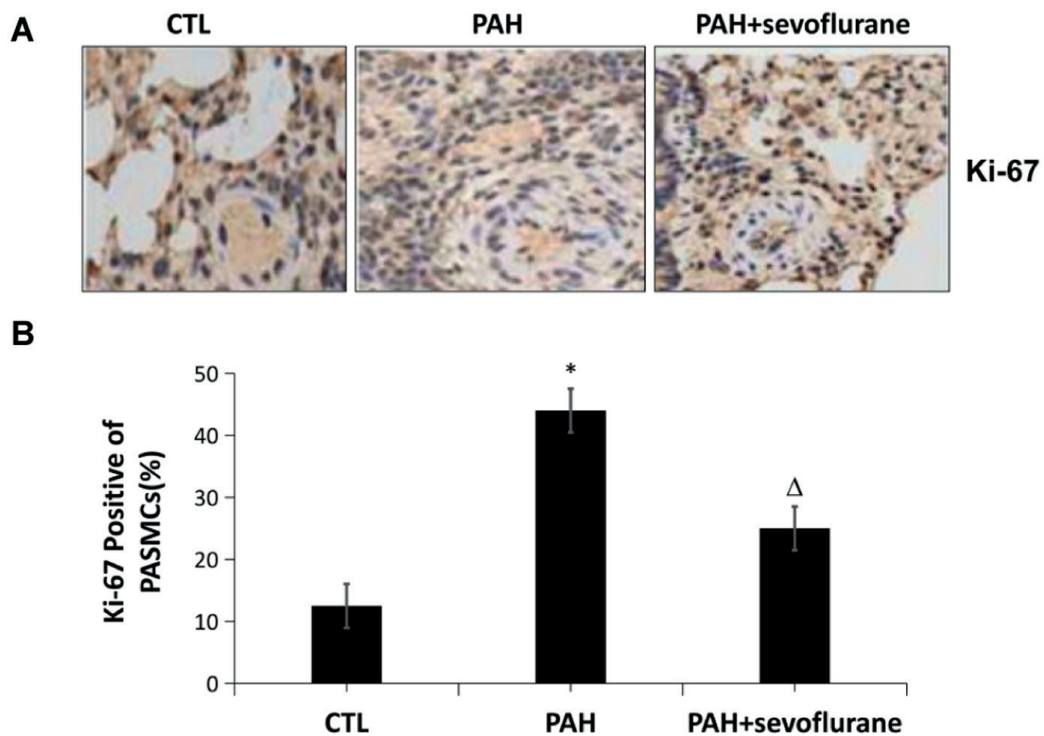
A

B

Figure 4. Ki-67 positive rate in pulmonary tissues. **A,** Immunohistochemical staining for measurement of Ki-67 positive rate in pulmonary arterial tissues (magnification × 40). **B,** Quantified Ki-67 positive rate in PASMCs. Note: Data were expressed as mean ± SEM, * PAH group *vs.* CTL group, $p<0.01$ and ᐃPAH + sevoflurane group *vs.* PAH group, $p<0.05$.

ever, these two indexes were smaller in PAH + sevoflurane group than those in PAH group. This suggested declined pulmonary arterial circulatory function in PAH group, which was mitigated by sevoflurane (Figure 7).

Discussion

PAH is a severe disease induced by pulmonary vascular morphological changes. In this process, hemodynamic disorder and endothelial dysfunc-

tion contribute to pulmonary arterial wall reconstruction and an increase in pulmonary vascular resistance. This further causes right heart dysfunction, ultimately leading to right heart failure in severe cases[10-14]. Garg et al[15] have demonstrated that persistent pulmonary vasoconstriction, vascular remodeling, and *in situ* thrombosis play a critical role in PAH.

Gene expression regulated by NF-κB manipulates many biological processes, such as the production of inflammatory factors, cell proliferation, and survival, differentiation of effector,
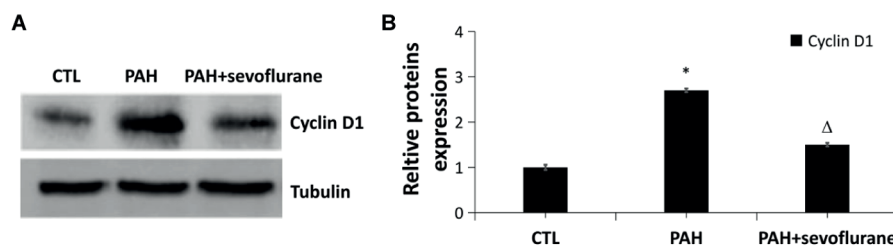
A

B

Figure 5. PASMC proliferation-related factors in pulmonary tissues. **A,** Western blotting results of cyclin D1 and tubulin expressions. **B,** Quantitative expressions of cyclin D1 and tubulin. Note: Data were expressed as mean ±SEM. * PAH group *vs.* CTL group, $p<0.01$, and ᐃPAH + sevoflurane group *vs.* PAH group, $p<0.05$.
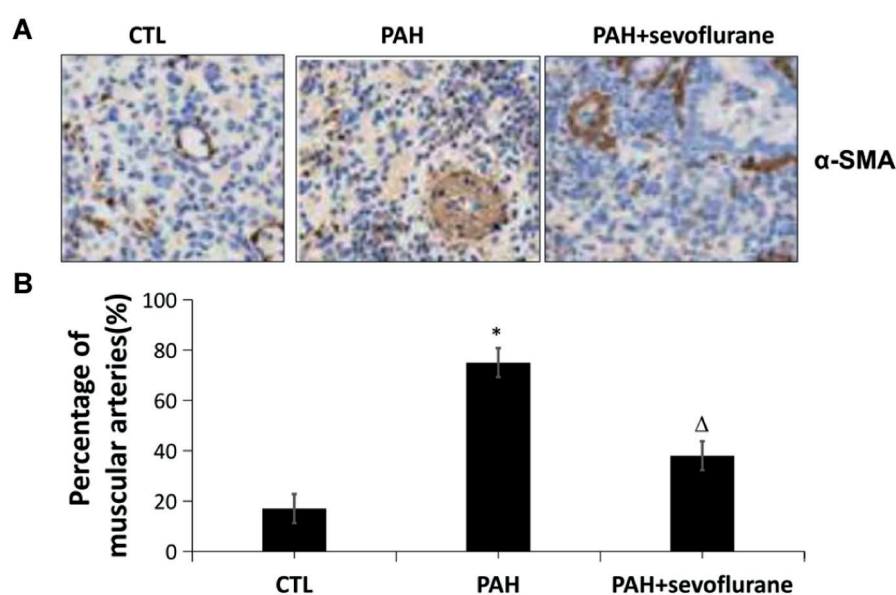
Figure 6. Pulmonary fibrosis in pulmonary tissues. **A,** Immunohistochemical staining for measurement of percentage of α-SMA in pulmonary artery fibrosis (magnification × 40). **B,** Quantified percentage of α-SMA in pulmonary artery fibrosis. Note: Data were expressed as mean ± SEM. * PAH group *vs.* CTL group, *p*<0.01, and ΔPAH + sevoflurane group *vs.* PAH group, *p*<0.05.

regulatory T cells, as well as the maturity of dendritic cells[16,17]. Therefore, the dysregulation of the NF-κB signaling pathway doubtlessly plays a crucial role in autoimmune diseases, including SLE and inflammatory diseases. Adu et al[18] have found that NF-κB signal transduction takes place in two different pathways. In canonical NF-κB signal transduction, downstream IκB of the IκB kinase (IKK) α/β/γ complex is degraded due to receptor activation. Subsequently, this may cause the translocation of the classical NF-κB subunits, such as P65 and P50, into cell nuclei to trigger immune gene expression. On the other hand, non-canonical NF-κB signal transduction strictly depends on the binding of NF-κB-inducing kinase (NIK, MAP3K14) to the tumor necrosis factor (TNF) receptor-associated factor 2/3 ubiquitin ligase complex. Meanwhile, the composition of this pathway is weakened by the continuous degradation of NIK proteins. TNFRSF signaling dissociates NIK from this complex, enabling it to accumulate. Furthermore, it phosphorylates IKKα, thereby phosphorylating NF-κB P100. As a result, P100 is cleaved to release mature transcription factor P52[19]. This is then dimerized with RelB and translocated into cell nuclei, initiating the transcription of the target gene.

In the present study, SD rats were assigned into three groups, namely CTL group, PAH group, and PAH + sevoflurane group. HE staining showed that compared with CTL group, rats in PAH group exhibited markedly thickened pulmonary arterial vascular wall and reduced the vascular lumen. This suggested that the PAH model was successfully established in rats. In PAH group, sevoflurane relieved the symptoms of PAH. The influence of sevoflurane on the NF-κB signaling pathway was then explored. Western blotting results demonstrated that the protein levels of p-IκB and p-P65 were significantly elevated in PAH group, thus activating the NF-κB signaling pathway. Since such activation was inhibited by sevoflurane, the mRNA expression of P65 was not substantially affected by various treatments. Subsequent immunohistochemistry of Ki-67 indicated that sevoflurane inhibited the proliferation of Ki-67-positive PASMCs. After that, PASMC proliferation-related factors were detected. Results manifested that the level of cyclin D1 was prominently upregulated in PAH group. Moreover, sevoflurane could down-regulate the level of cyclin D1 and up-regulate the level of proliferating cell nuclear antigen (PCNA). These findings were similar to immunohistochemical detection results of Ki-67. Additionally, immunohistochemical detection results of α-SMA revealed that sevoflurane inhibited the increase in α-SMA in pulmonary tissues, thus inhibiting arterial vascular
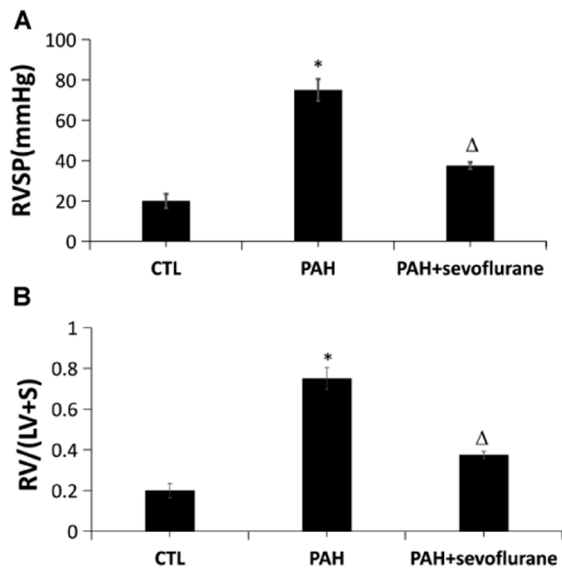
Figure 7. Detection results of pulmonary arterial circulatory function-related indicators. Blood sample was collected to detect RVSP (**A**) and RVHI (**B**). Note: Data were expressed as mean ± SEM. * PAH group, *p*<0.01 *vs.* CTL group, and $^\Delta$PAH + sevoflurane group *vs.* PAH group, *p*<0.05.

fibrosis. Further results illustrated that RVSP and RVHI were down-regulated by sevoflurane, thus preventing PAH.

Conclusions

We first observed that sevoflurane could lower the levels of p-IκB, p-P65, and P65 to repress the activation of NF-κB signaling pathway and inhibit PASMC proliferation in pulmonary tissues. This might reduce pulmonary fibrosis and ultimately prevent PAH. Furthermore, these findings suggested a positive role of sevoflurane in the prevention and treatment of PAH.

Conflict of Interests

The Authors declare that they have no conflict of interests.

References

1) Keating GM. Macitentan: a review in pulmonary arterial hypertension. Am J Cardiovasc Drugs 2016; 16: 453-460.

2) Liu Z, Duan YL, Ge SL, Zhang CX, Gong WH, Xu JJ. Effect of estrogen on right ventricular remodeling of monocrotaline-induced pulmonary arterial hypertension in rats and its mechanism. Eur Rev Med Pharmacol Sci 2019; 23: 1742-1750.

3) Simonneau G, Channick RN, Delcroix M, Galie N, Ghofrani HA, Jansa P, Le Brun FO, Mehta S, Perchenet L, Pulido T, Sastry BK, Sitbon O, Souza R, Torbicki A, Rubin LJ. Incident and prevalent cohorts with pulmonary arterial hypertension: insight from SERAPHIN. Eur Respir J 2015; 46: 1711-1720.

4) Weiss A, Neubauer MC, Yerabolu D, Kojonazarov B, Schlueter BC, Neubert L, Jonigk D, Baal N, Ruppert C, Dorfmuller P, Pullamsetti SS, Weissmann N, Ghofrani HA, Grimminger F, Seeger W, Schermuly RT. Targeting cyclin-dependent kinases for the treatment of pulmonary arterial hypertension. Nat Commun 2019; 10: 2204.

5) Cao X, He Y, Li X, Xu Y, Liu X. The IRE1alpha-XBP1 pathway function in hypoxia-induced pulmonary vascular remodeling, is upregulated by quercetin, inhibits apoptosis and partially reverses the effect of quercetin in PASMCs. Am J Transl Res 2019; 11: 641-654.

6) Yang L, Xie P, Wu J, Yu J, Yu T, Wang H, Wang J, Xia Z, Zheng H. Sevoflurane postconditioning improves myocardial mitochondrial respiratory function and reduces myocardial ischemia-reperfusion injury by up-regulating HIF-1. Am J Transl Res 2016; 8: 4415-4424.

7) Pasqualin RC, Mostarda CT, Souza LE, Vane MF, Sirvente R, Otsuki DA, Torres ML, Irigoyen MC, Auler JO Jr. Sevoflurane preconditioning during myocardial ischemia-reperfusion reduces infarct size and preserves autonomic control of circulation in rats. Acta Cir Bras 2016; 31: 338-345.

8) Wang G, Liu J, Gao J, Zheng X. Comparison of the effects of sevoflurane and propofol anesthesia on pulmonary function, MMP-9 and postoperative cognition in patients receiving lung cancer resection. Oncol Lett 2019; 17: 3399-3405.

9) Zhou T, Guo S, Wang S, Li Q, Zhang M. Protective effect of sevoflurane on myocardial ischemia-reperfusion injury in rat hearts and its impact on HIF-1alpha and caspase-3 expression. Exp Ther Med 2017; 14: 4307-4311.

10) Hoeper MM, Ghofrani HA, Grunig E, Klose H, Olschewski H, Rosenkranz S. Pulmonary hypertension. Dtsch Arztebl Int 2017; 114: 73-84.

11) van Dissel AC, Mulder BJ, Bouma BJ. The changing landscape of pulmonary arterial hypertension in the adult with congenital heart disease. J Clin Med 2017; 6. pii: E40.

12) Nashat H, Brida M, Price LS, McCabe C, Alonso-Gonzalez R, Wort SJ, Kempny A, Dimopoulos K, Gatzoulis MJ. Pulmonary arterial hypertension complicating congenital heart disease: advances in therapy. Semin Respir Crit Care Med 2017; 38: 636-650.

13) Liu M, Qin C, Xia X, Li M, Wang Y, Wang L, Shang X, Lan X. Semi-quantitative assessment of pulmonary arterial hypertension associated with congenital heart disease through myocardial

perfusion imaging. Hell J Nucl Med 2017; 20: 204-210.

14) Vonk-Noordegraaf A, Haddad F, Chin KM, Forfia PR, Kawut SM, Lumens J, Naeije R, Newman J, Oudiz RJ, Provencher S, Torbicki A, Voelkel NF, Hassoun PM. Right heart adaptation to pulmonary arterial hypertension: physiology and pathobiology. J Am Coll Cardiol 2013; 62 (25 Suppl): D22-D33.

15) Garg L, Akbar G, Agrawal S, Agarwal M, Khaddour L, Handa R, Garg A, Shah M, Patel B, Dalal BD. Drug-induced pulmonary arterial hypertension: a review. Heart Fail Rev 2017; 22: 289-297.

16) Kawamura N, Kubota T, Kawano S, Monden Y, Feldman AM, Tsutsui H, Takeshita A, Sunagawa K. Blockade of NF-kappaB improves cardiac function and survival without affecting inflammation in TNF-alpha-induced cardiomyopathy. Cardiovasc Res 2005; 66: 520-529.

17) Newton K, Sun X, Dixit VM. Kinase RIP3 is dispensable for normal NF-kappa Bs, signaling by the B-cell and T-cell receptors, tumor necrosis factor receptor 1, and Toll-like receptors 2 and 4. Mol Cell Biol 2004; 24: 1464-1469.

18) Adli M, Merkhofer E, Cogswell P, Baldwin AS. IKKalpha and IKKbeta each function to regulate NF-kappaB activation in the TNF-induced/canonical pathway. PLoS One 2010; 5: e9428.

19) Xiao G, Fong A, Sun SC. Induction of p100 processing by NF-kappaB-inducing kinase involves docking IkappaB kinase alpha (IKKalpha) to p100 and IKKalpha-mediated phosphorylation. J Biol Chem 2004; 279: 30099-30105.